

## *Aging and Reversion in Dilute Al-Ag Alloys*

Mutsuo OHTA\*, Teruto KANADANI\*\*, Masuo YAMADA\* and  
Akira SAKAKIBARA\*

(Received January 31, 1979)

### Synopsis

Aging and reversion in dilute Al-Ag alloys are studied by means of the measurements of electrical resistivity. Results obtained are as follows:

1) Increase in the as-quenched resistivity is found for a low quenching temperature. This increase may be due to the fluctuation of solute concentration at the quenching temperature.

2) When the fluctuation exists in the alloy, the aging rate becomes slow and the maximum resistivity in the isothermal aging curve becomes small as the vacancy concentration becomes low. The maximum resistivity becomes large again when the vacancy concentration becomes further lower, and finally the maximum does not appear.

3) These behaviors are explained in terms of the difference in the rate of growth of the G.P. zones in the regions of higher and lower solute concentration induced by the fluctuation and in terms of the change of this difference with vacancy concentration.

4) G.P. zones may be formed by the spinodal decomposition with indefinite surfaces at first, grown to larger ones with definite surfaces and changed to ordered  $\eta$ -zones in the alloy.

5) It is confirmed that G.P. zones are formed by the

---

\* Department of industrial Science.

\*\* Okayama University of Science.

nucleation-and-growth mechanism also in Al-Ag alloys above the spinodal temperature.

## 1. Introduction

Al-Ag alloys, typical age-hardenable alloys, have been studied by various methods. In most of the studies, alloys of high concentration in which G.P. zones were formed and grown rapidly have been used and, hence, little has been known on the details of the initial process of aging.

It has been suggested that fluctuation of solute concentration exists at temperatures higher than the spinodal temperature in the solid solution of Al-Zn alloys (1-3). Al-Ag alloys exhibit aging behaviors similar to Al-Zn alloy, but the existence of fluctuation and its effects on the low-temperature aging has not been found experimentally in low concentrated Al-Ag alloys.

It has been also reported (4,5) on Al-Zn alloys that G.P. zones are formed by the nucleation-and-growth mechanism at the temperature higher than the spinodal temperature, but no study but one by X-ray measurements was reported on the mechanism in Al-Ag alloys (6).

In this report, aging and reversion in dilute Al-Ag alloys are studied by means of the measurements of electrical resistivity. Dilute alloys are appropriate for studying the process of aging and reversion because of their slow aging rate and low spinodal temperature.

## 2. Experimental Procedures

### 2.1 Specimens

The alloys used were, nominally, Al-0.1, 0.3, 0.45, 1.0, 1.5, 5.0wt%Ag and pure metals used to make these alloys were 99.996% Al and 99.9% Ag. Alloys were cast into metallic mold in air. The ingots were homogenized at 500°C for 50hr, hot-forged to sheets of 5mm in thickness and cold-rolled to strips of 0.4mm in thickness. Specimens for resistivity measurements were cut off from these strips, the main part of them being 0.7mm wide and 70mm long with four long leads of the same alloy.

### 2.2 Heat Treatments

Quenching method was the same as in a previous report (7). Main part of the specimen was set in the narrow opening (3mm wide and 50mm

deep) of the aluminium block (50mm in diameter and 100mm in length) installed in the furnace, lead parts being attached closely to the aluminium block. Specimen was held at 500°C for 1hr, cooled (or heated) in the furnace to the quenching temperature and held there for 1hr. Quenching was carried out by hand by extracting the specimen quickly out of the furnace and immersing it into iced water bath. Then it was transferred into liquid nitrogen as quickly as possible. Maximum cooling rate in this method of quenching was about 8000°C/sec when the quenching temperature was 350°C or so. It took, however, about 3sec to reach liquid-nitrogen temperature from 0°C, so G.P. zones were unavoidably formed between -20°C and -60°C when the quenching temperature was high.

Annealing was carried out in ethanol, water or silicon-oil bath, each for its proper temperature range. Silicon-oil bath was used to avoid corrosion when the annealing time was long.

### 2.3 Resistivity Measurements

Electrical resistivity was measured by a usual potentiometric method, specimens being held in liquid nitrogen. Effect of the temperature of liquid nitrogen on the resistivity was corrected by using a well-annealed dummy of the alloy whose composition was the same as that of the specimen. Specific resistivity was calculated from the dimension and weight of the main part of the specimen which was cut off after the measurement of resistivity.

### 3. Results

In Fig.1, variation of as-quenched resistivity ( $\rho_0$ ) with quenching temperature ( $T_Q$ ) is shown. As was observed in Al-Zn alloys (8),  $\rho_0$  is high in the lower and higher temperature range and takes a minimum value at the intermediate temperature which is determined uniquely by the composition. When the curves of the alloys are compared with the curve of pure Al in the figure, increase of  $\rho_0$  above 200°C in the curves of the alloys can be attributed mainly to the contribution of quenched vacancies, and partly to that of G.P. zones which may be formed during the cooling process, especially during the slow cooling under 0°C in liquid nitrogen bath. Increase of  $\rho_0$  at lower  $T_Q$  can be attributed to the fluctuation of solute concentration existing at  $T_Q$ , as was the case in Al-Zn alloys.

Figure 2 shows isothermal aging curves of the Al-0.3wt%Ag alloy at 0°C after quenching from various temperatures. In all curves

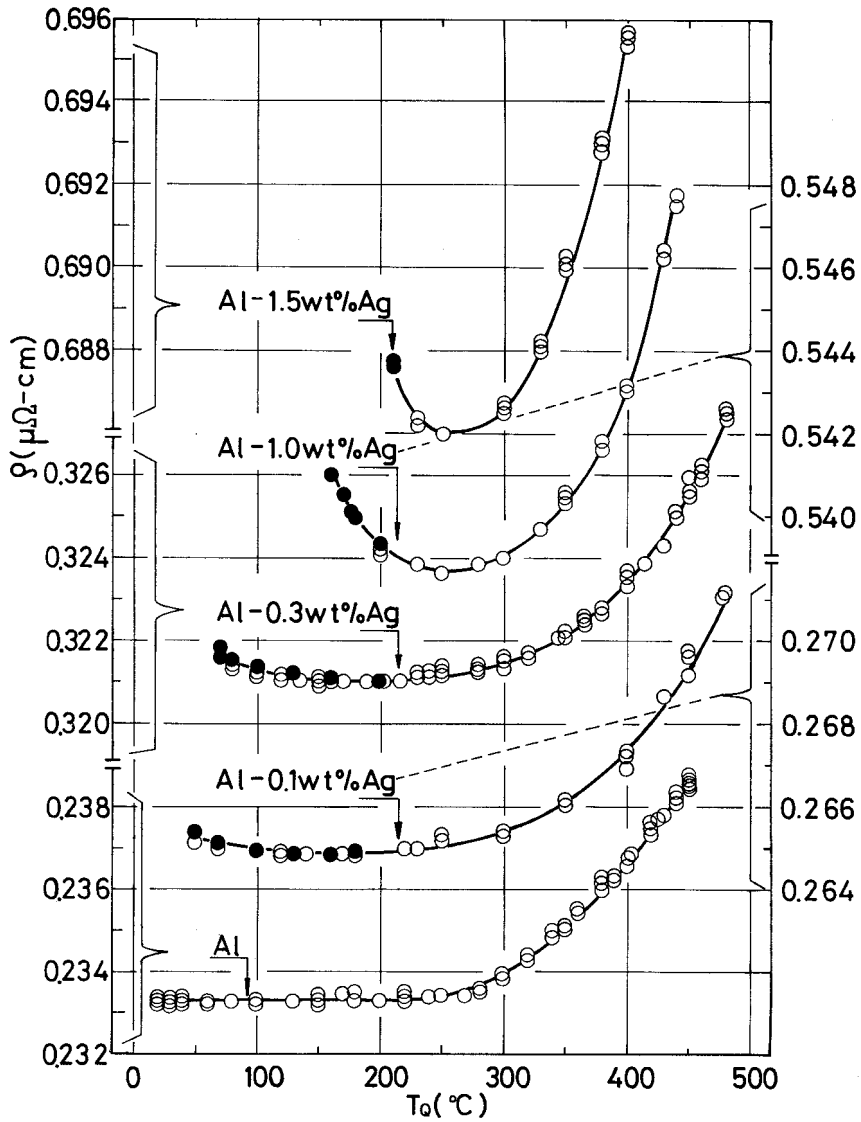


Fig.1 The variation of as-quenched resistivity( $\rho_0$ ) with quenching temperature( $T_Q$ ).

● : quasi-equilibrium resistivities when the alloys were annealed at the temperature of the abscissa after quenching from 300°C to 0°C. These values coincide well with  $\rho_0$  at each temperature.

except the one for  $T_Q=200^\circ\text{C}$  the resistivity increases at first, reaches the maximum and then decreases as aging proceeds. Figure 3 shows isothermal aging curves of the Al-1.0wt%Ag alloy at 0°C after quenching from various temperatures. In Fig.4, the maximum resistivity( $\rho_{\max}$ ) in the isothermal curves are plotted against  $T_Q$ . For the

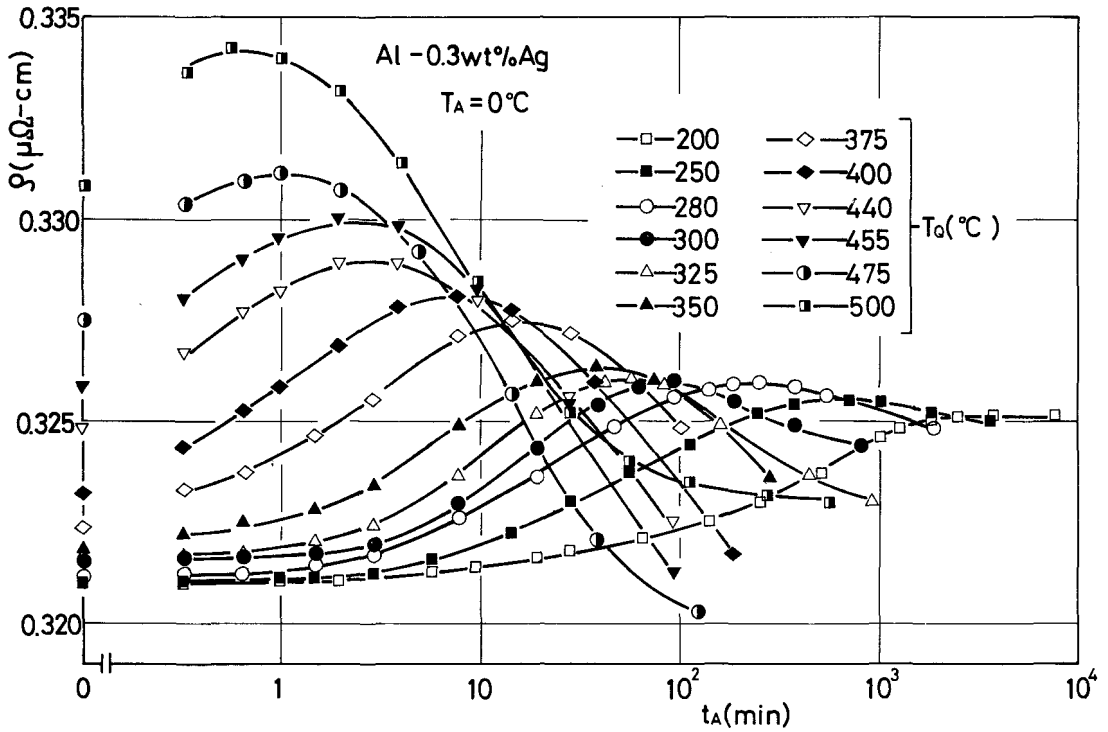


Fig.2 Isothermal aging curves of the Al-0.3wt%Ag alloy at  $0^\circ\text{C}$  for various  $T_Q$ .

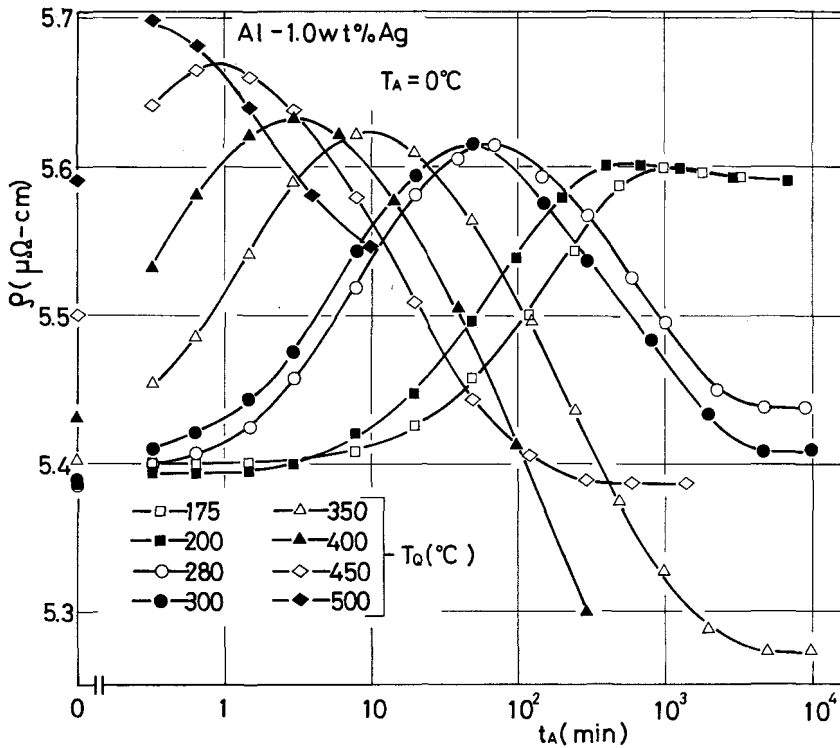


Fig.3 Isothermal aging curves of the Al-1.0wt%Ag alloy at  $0^\circ\text{C}$  for various  $T_Q$ .

Al-0.3wt%Ag alloy,  $\rho_{\max}$  is constant in the temperature range between 280 and 325°C, but it increases with increasing  $T_Q$  above 350°C and decreases with decreasing  $T_Q$  below 250°C. These features were also found in Al-Zn alloys (8).

Figure 5 shows isothermal aging curves of the Al-0.3wt%Ag alloy at 50°C. As has been previously reported by one of the present authors (9), maximum resistivity in the isothermal aging curve was recognized upto the aging temperature 70°C. For the Al-Zn alloy, it was found experimentally (5,10) that the spinodal decomposition was accompanied by the resistivity maximum in the isothermal aging curve. Therefore, spinodal tempera-

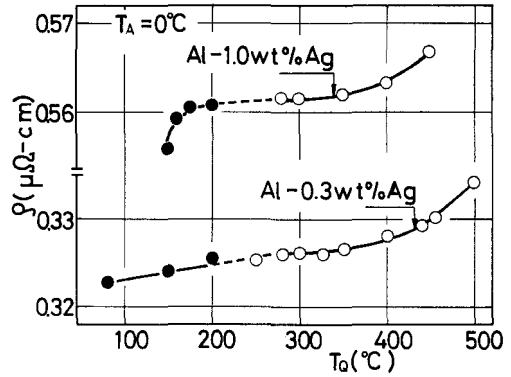


Fig.4  $\rho_{\max}$  (the maximum resistivity in the aging curve) vs.  $T_Q$  plots.

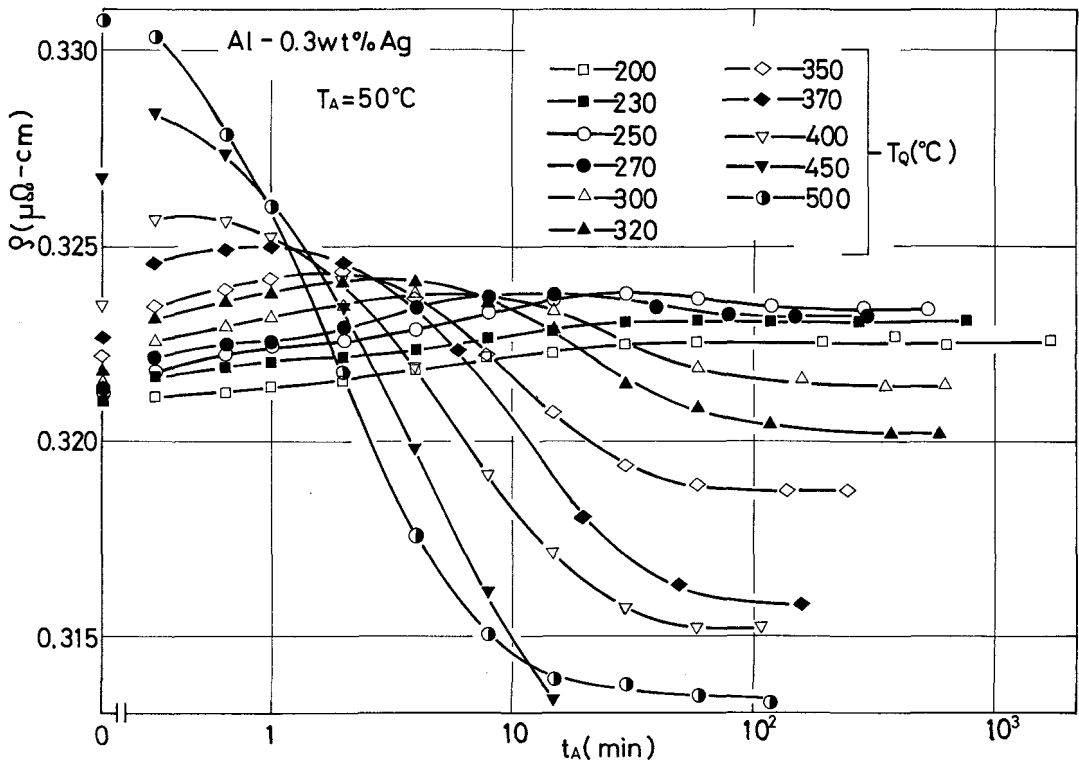


Fig.5 Isothermal aging curves of the Al-0.3wt%Ag alloy at 50°C for various  $T_Q$ .

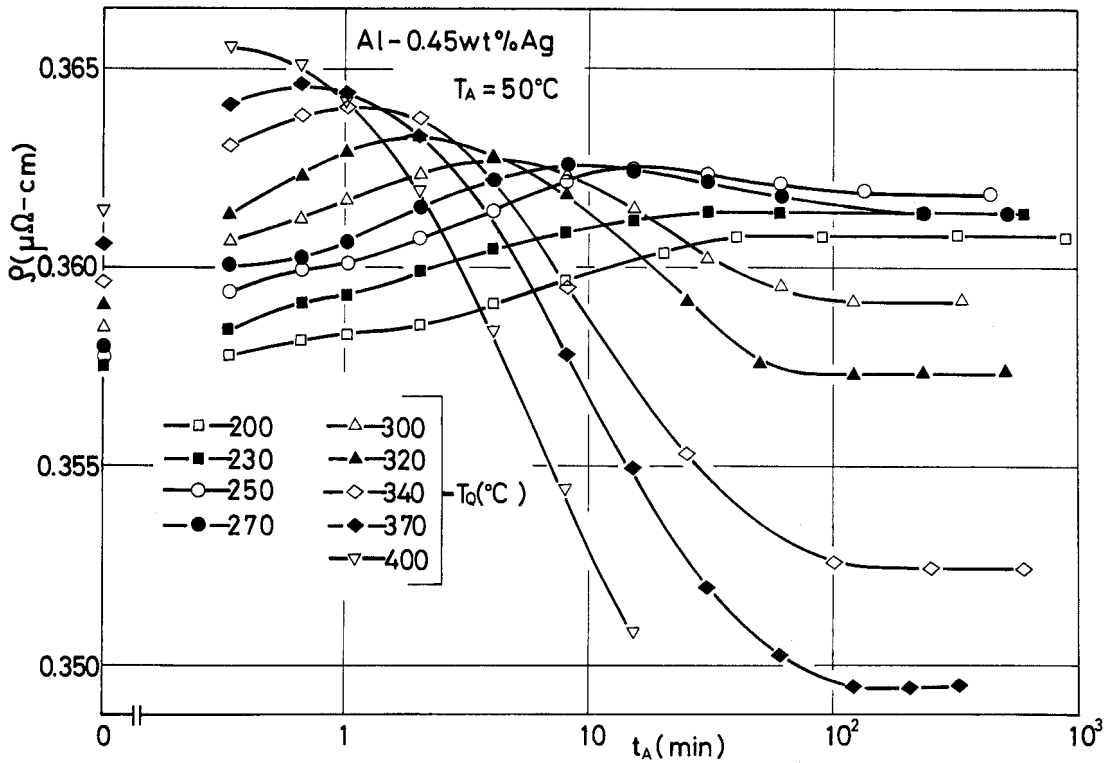


Fig.6 Isothermal aging curves of the Al-0.45wt%Ag alloy at  $50^\circ\text{C}$  for various  $T_Q$ .

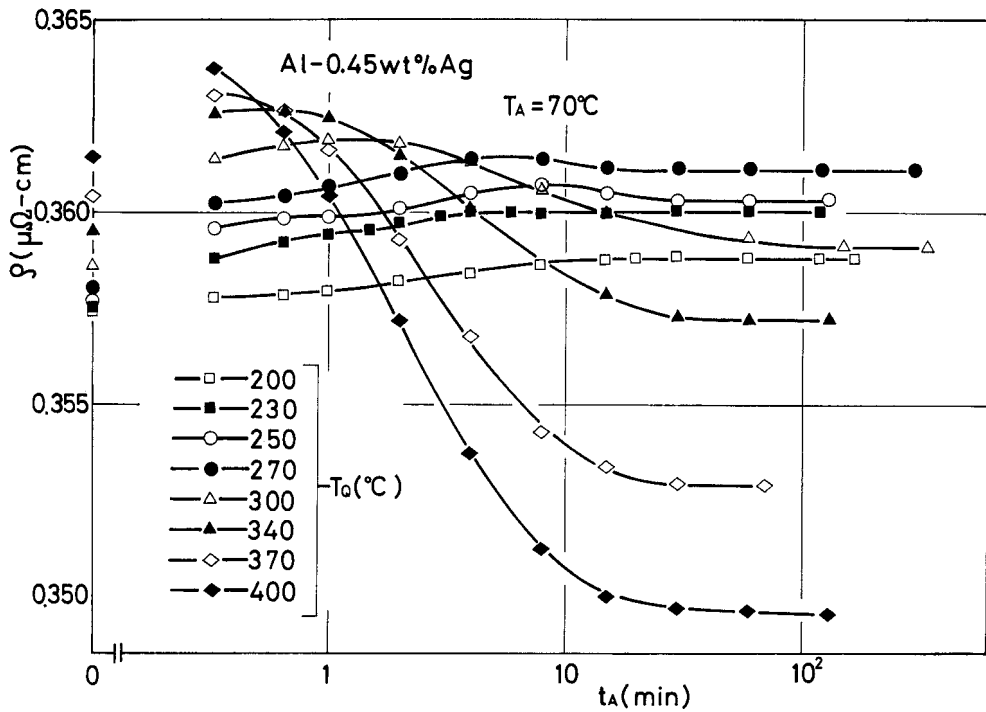


Fig.7 Isothermal aging curves of the Al-0.45wt%Ag alloy at  $70^\circ\text{C}$  for various  $T_Q$ .

ture of the Al-0.3wt%Ag alloy is considered to be about 70°C. Hence, aging temperature 50°C was employed because of the small driving force of the spinodal decomposition at the temperature. These aging curves as a whole resemble those obtained on aging at 0°C. When  $T_Q$  is 250 or 230°C, however, resistivity almost stops to increase temporarily before the maximum and then increases again, that is, two-step increase is observed. When  $T_Q$  is 230 or 200°C, resistivity increases gradually, reaches a stationary value without taking maximum, and remains there for a long time. Figures 6 and 7 show similar results of the Al-0.45wt%Ag alloy.

Isothermal aging curves obtained are shown in Figs. 8-18 for alloys of various concentration and for various  $T_{Q1}$ ,  $T_{Q2}$  and  $T_A$ . In all figures, the time elapsed until the maximum resistivity attained becomes longer as the time at  $T_{Q2}$  increases. The shape of most curves is an ordinary one; the resistivity increases initially, reaches the maximum, and then decreases. But several curves are different; a few curves show the "two-step" increase of the resistivity and the others does not reach the maximum in the usual aging period. The values of the maximum resistivity in the isothermal aging curves for the alloy of a certain concentration vary with  $T_{Q2}$  and the holding time at  $T_{Q2}$ .

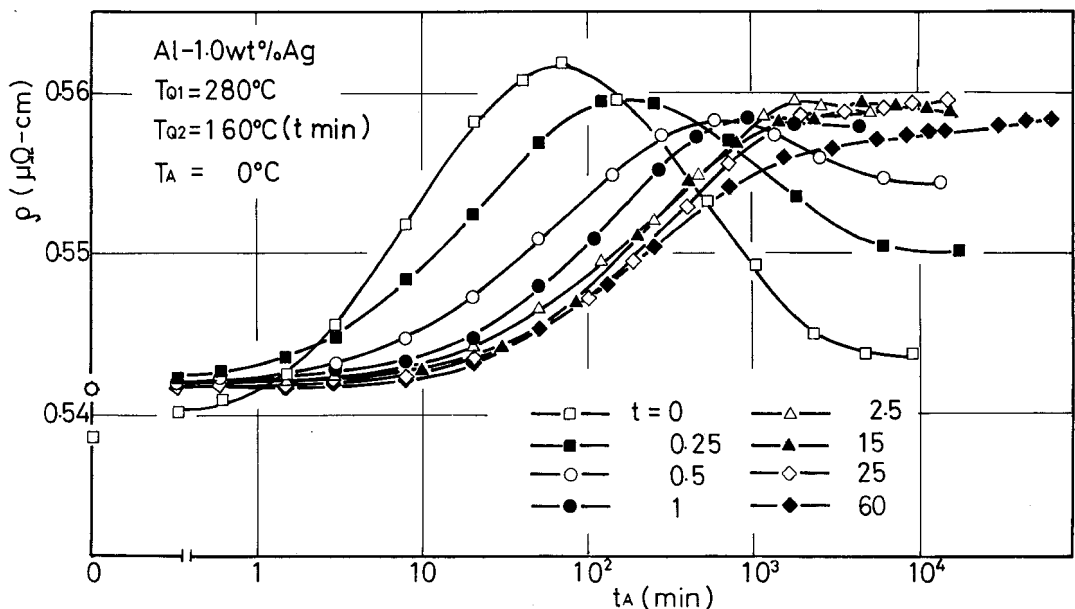


Fig.8 Aging curves of the 1.0%Ag alloy at 0°C.  $T_{Q1}=280^\circ\text{C}$ .  $T_{Q2}=160^\circ\text{C}$  for  $t$  min.



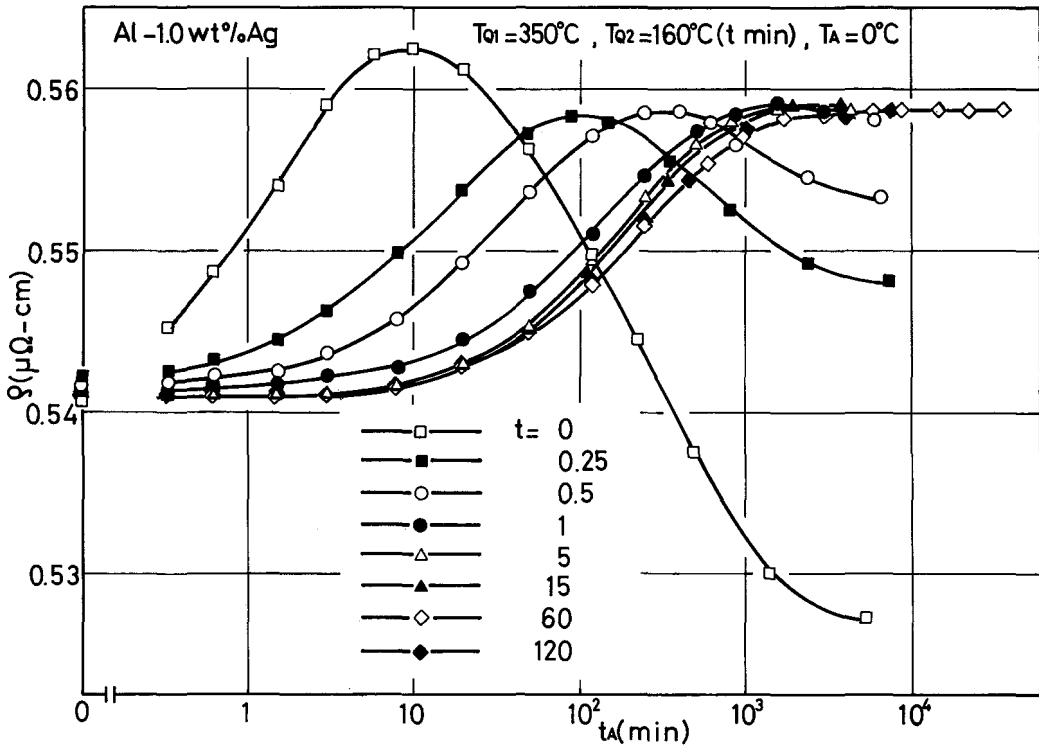


Fig.9 Aging curves of the 1.0%Ag alloy at 0°C.  $T_{Q1}=350^{\circ}\text{C}$ .  $T_{Q2}=160^{\circ}\text{C}$  for t min.

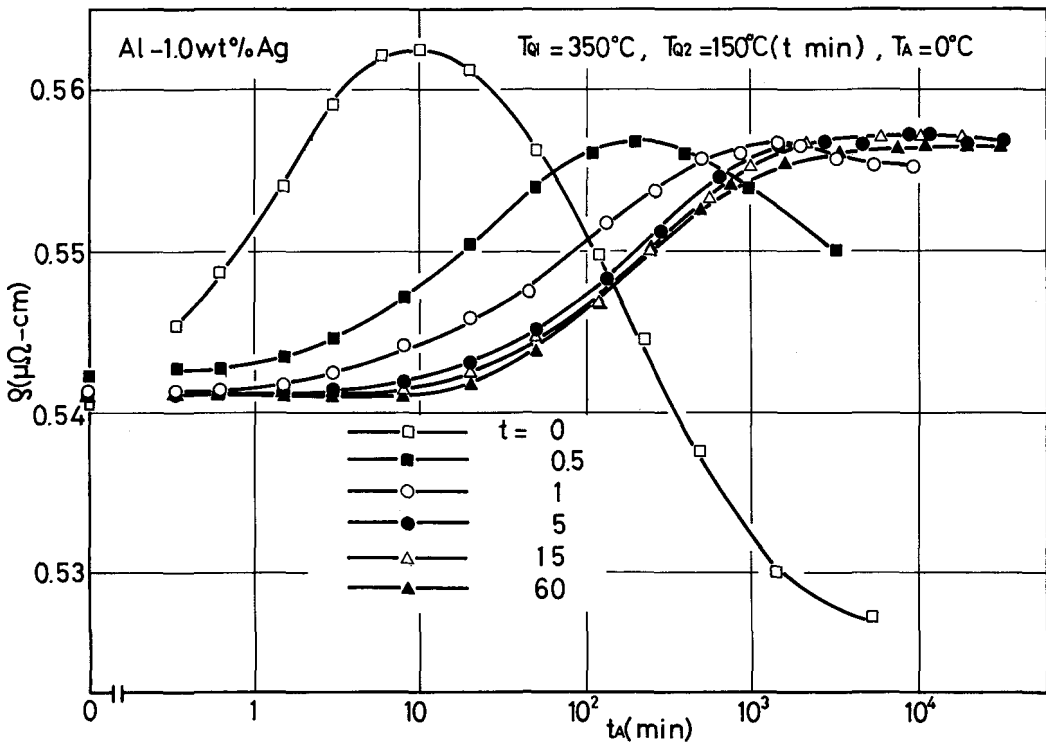


Fig.10 Aging curves of the 1.0%Ag alloy at 0°C.  $T_{Q1}=350^{\circ}\text{C}$ .  $T_{Q2}=150^{\circ}\text{C}$  for t min.

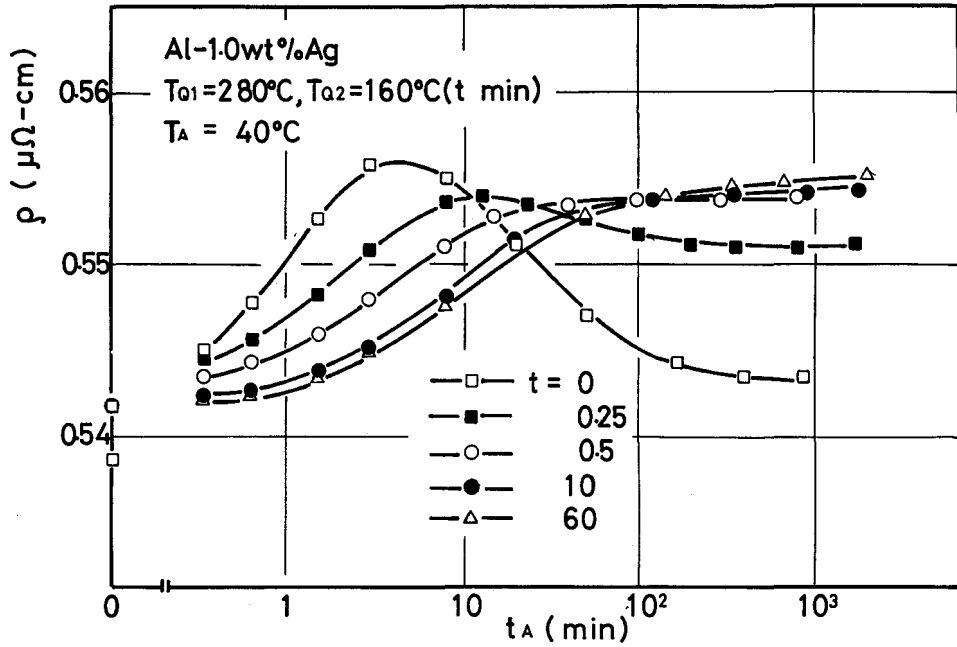


Fig.11 Aging curves of the 1.0%Ag alloy at  $40^{\circ}\text{C}$ .  $T_{Q1}=280^{\circ}\text{C}$ .  $T_{Q2}=160^{\circ}\text{C}$  for  $t$  min.

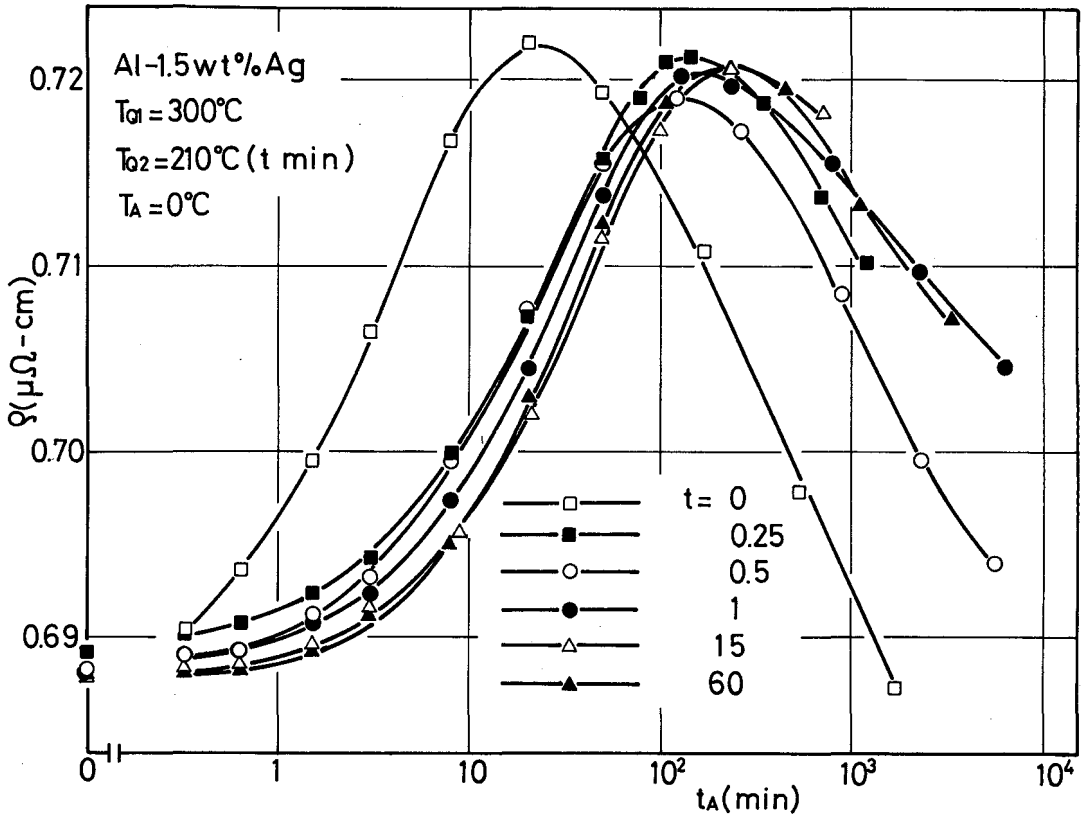


Fig.12 Aging curves of the 1.5%Ag alloy at  $0^{\circ}\text{C}$ .  $T_{Q1}=300^{\circ}\text{C}$ .  $T_{Q2}=210^{\circ}\text{C}$  for  $t$  min.

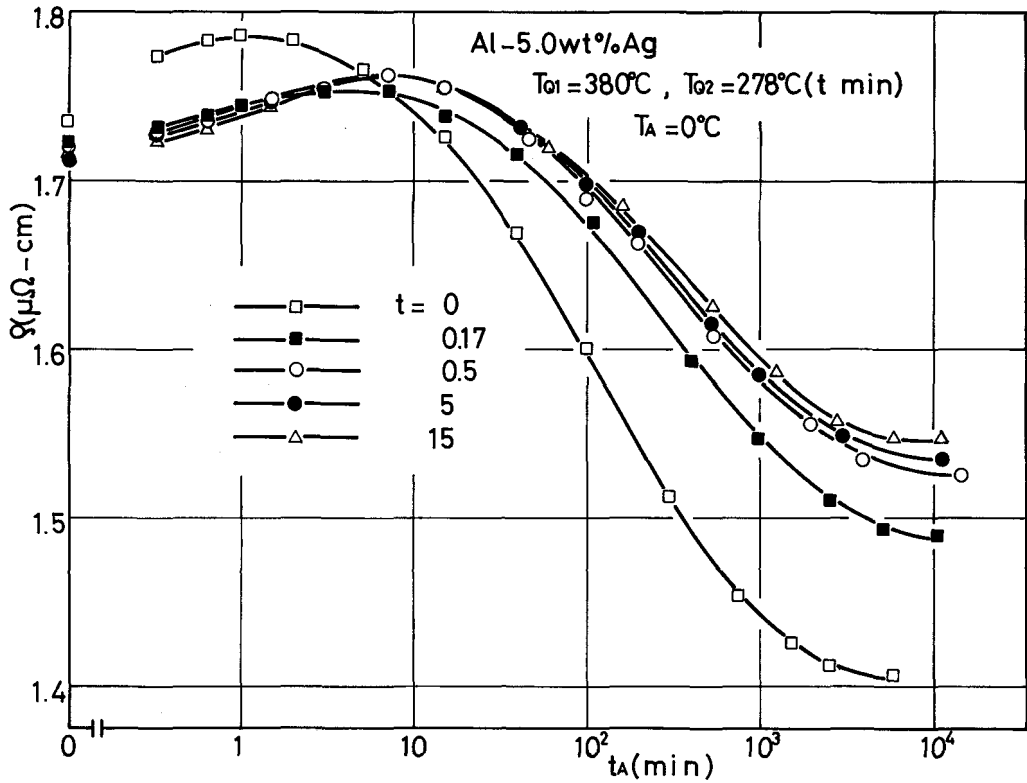


Fig.13 Aging curves of the 5.0%Ag alloy at 0°C.  $T_{Q1}=380^{\circ}\text{C}$ .  $T_{Q2}=278^{\circ}\text{C}$  for  $t$  min.

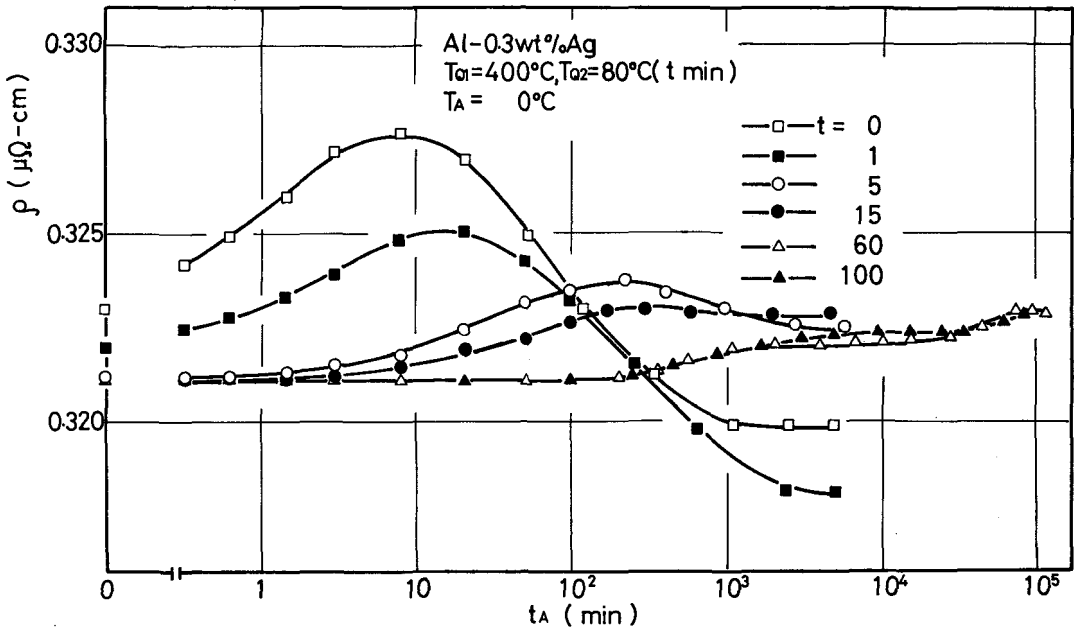


Fig.14 Aging curves of the 0.3%Ag alloy at 0°C.  $T_{Q1}=400^{\circ}\text{C}$ .  $T_{Q2}=80^{\circ}\text{C}$  for  $t$  min.

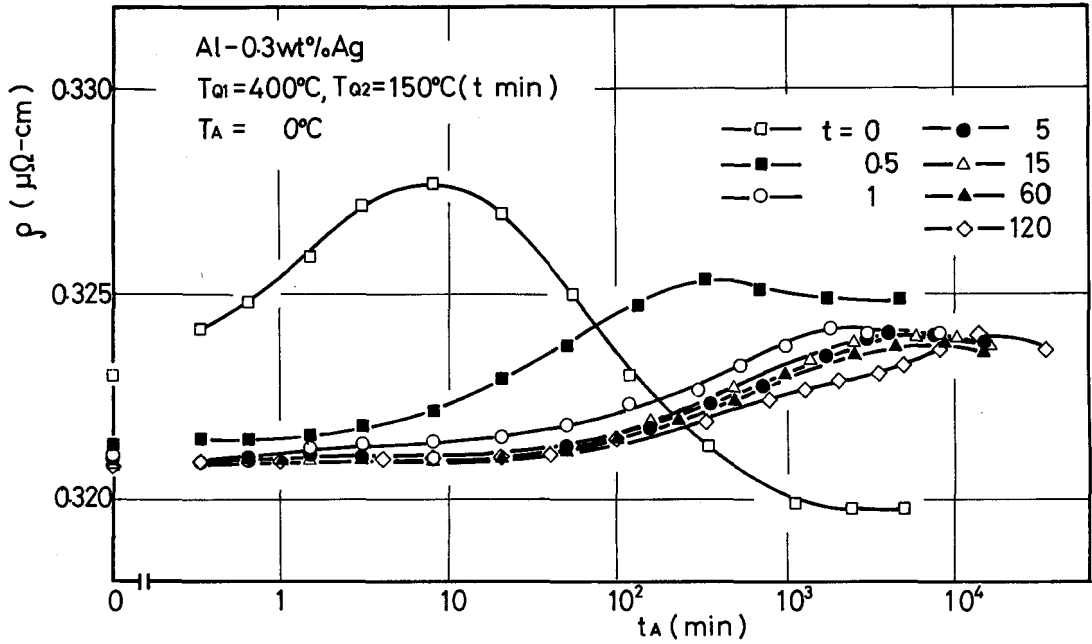


Fig.15 Aging curves of the 0.3%Ag alloy at  $0^{\circ}\text{C}$ .  $T_{Q1}=400^{\circ}\text{C}$ .  $T_{Q2}=150^{\circ}\text{C}$  for  $t$  min.

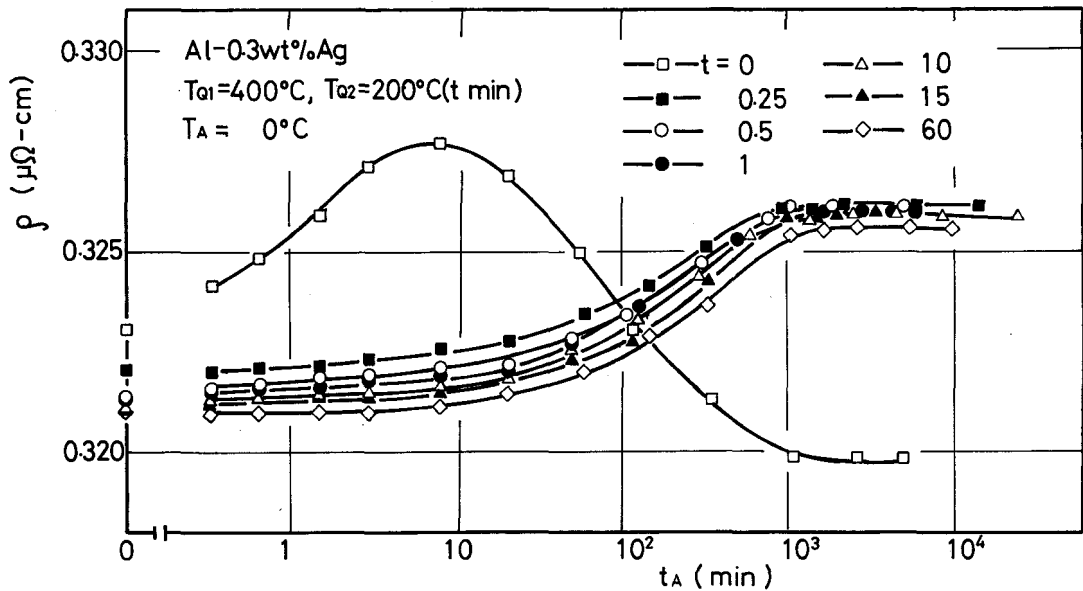


Fig.16 Aging curves of the 0.3%Ag alloy at  $0^{\circ}\text{C}$ .  $T_{Q1}=400^{\circ}\text{C}$ .  $T_{Q2}=200^{\circ}\text{C}$  for  $t$  min.

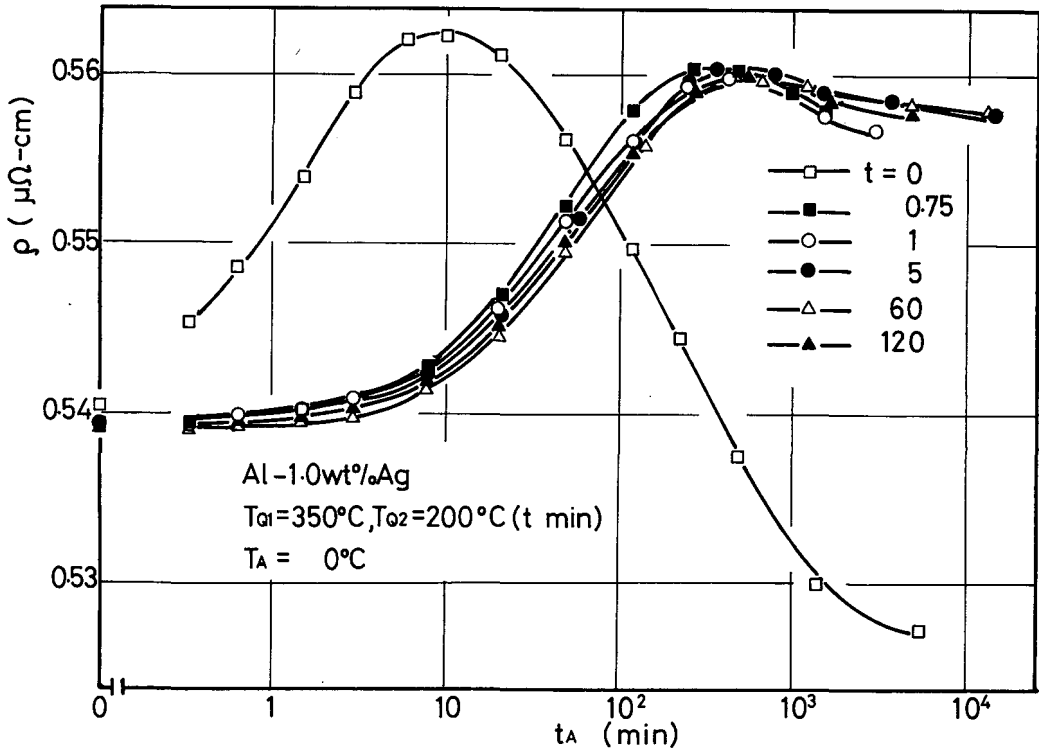


Fig.17 Aging curves of the 1.0%Ag alloy at  $0^{\circ}\text{C}$ .  $T_{Q1}=350^{\circ}\text{C}$ .  $T_{Q2}=200^{\circ}\text{C}$  for t min.

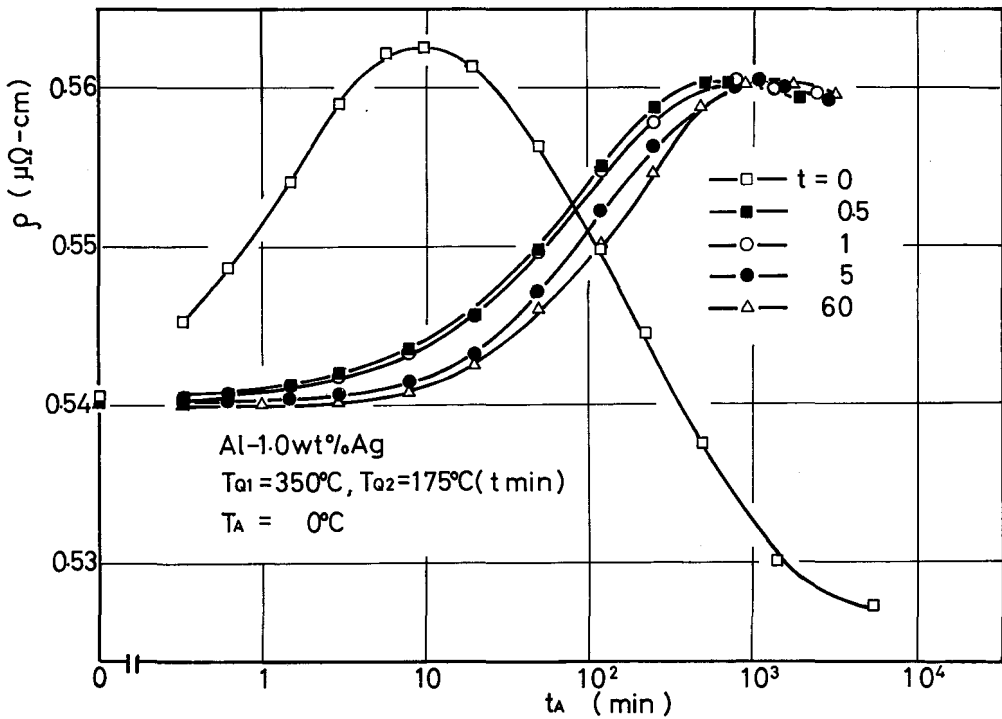


Fig.18 Aging curves of the 1.0%Ag alloy at  $0^{\circ}\text{C}$ .  $T_{Q1}=350^{\circ}\text{C}$ .  $T_{Q2}=175^{\circ}\text{C}$  for t min.

The maximum resistivity in the isothermal aging curves plotted against the holding time at the intermediate temperature ( $T_{Q2}$ ) are shown in Figs. 19~21. In rather high-concentrated alloys and low  $T_{Q2}$ , maximum resistivity decreases at first, takes a minimum value and then increases to a stationary value with increasing holding time (Figs. 8~13). The stationary value is smaller than that obtained when the specimen was quenched directly from a higher quenching temperature. For rather low-concentrated alloys and high  $T_{Q2}$ , the resistivity decreases at first and reaches a stationary value with increasing holding time at  $T_{Q2}$ , having no minimum value (Figs. 14~18).

Isochronal annealing was carried out for several specimens after the isothermal aging mentioned above. The results are shown in Figs. 22~24. When the Al-0.3wt%Ag alloy was quenched from 270°C and aged at 50°C for 10, 80 and 840min, isochronal annealing for 2min at intervals of 5°C indicates rapid decrease of resistivity in the range of 70~80°C, 90~105°C and 120~135°C (Fig.22). It is considered that the lower two stages in these reversion is the same as that observed

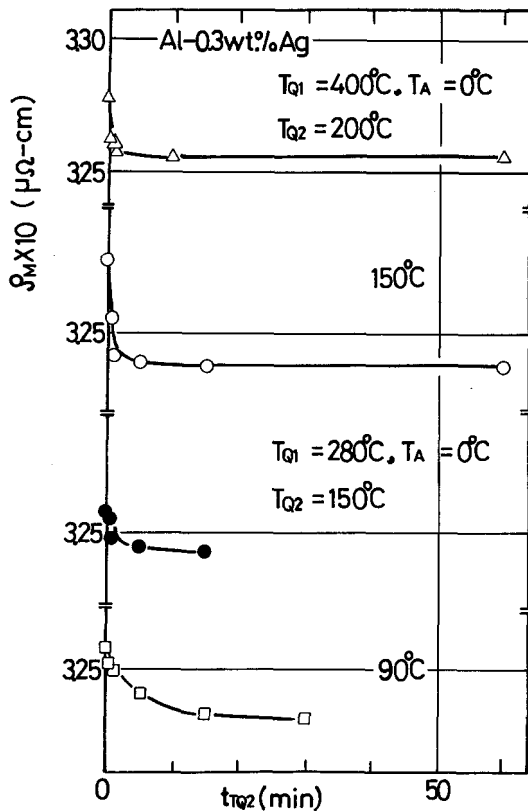


Fig.19 Variation of  $\rho_{max}$  with the holding time at  $T_{Q2}$  for 0.3%Ag alloy.

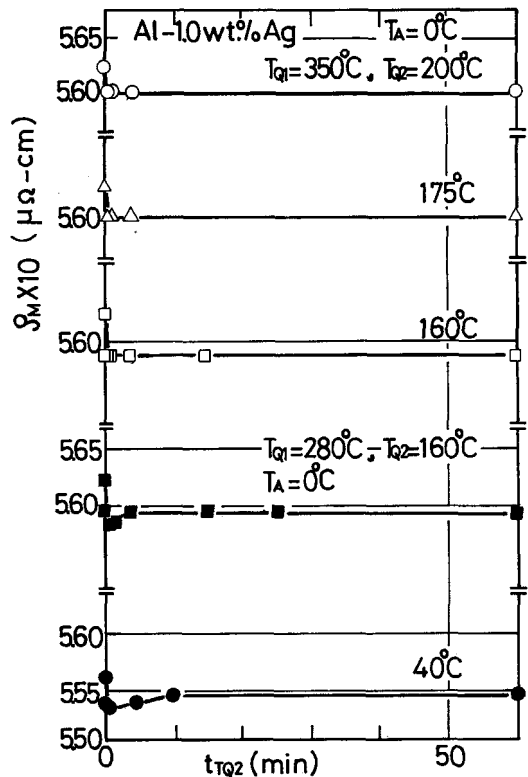


Fig.20 Variation of  $\rho_{max}$  with the holding time at  $T_{Q2}$  for 1.0%Ag alloy.

in the dilute Al-Zn alloys, and that the third stage is inherent in the Al-Ag alloys. In Fig.22 an isochronal annealing curve is shown also for the same alloy aged at 50°C for 100min after quenching from 400°C into iced water. Two stages of increase of resistivity is observed in the isochronal annealing, the lower one being around 110°C corresponding to the 2nd stage of the above case and the higher one being between 125 and 155°C corresponding to the 3rd stage above. Resistivity change below the spinodal temperature is represented with broken lines in the figure because this change is not regarded simply as the decay

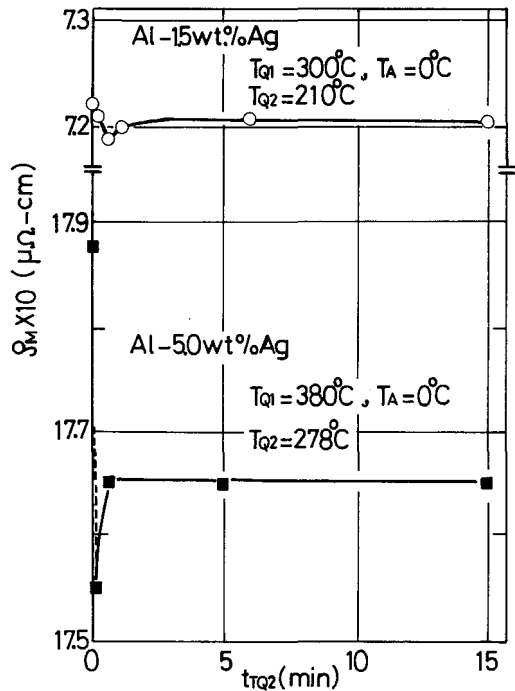


Fig.21  $\rho_{max}$  vs. holding time at  $T_{Q2}$ .

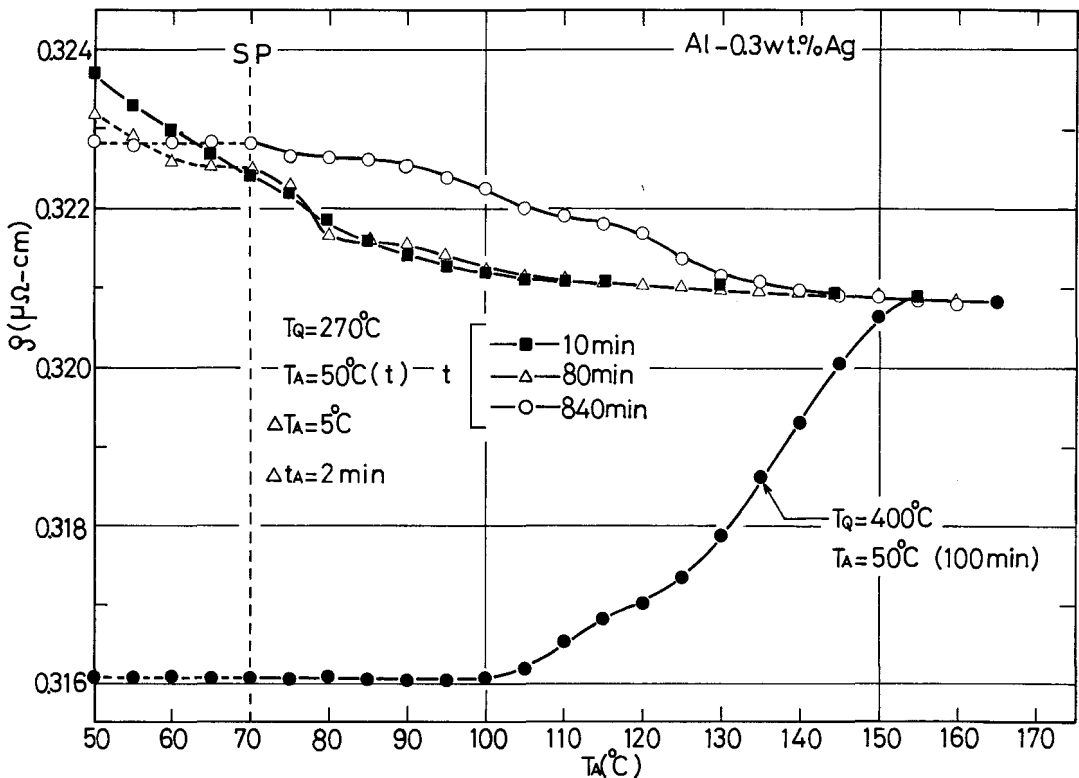


Fig.22 Isochronal curves of the 0.3%Ag alloy aged at 50°C for various  $t_A$ .

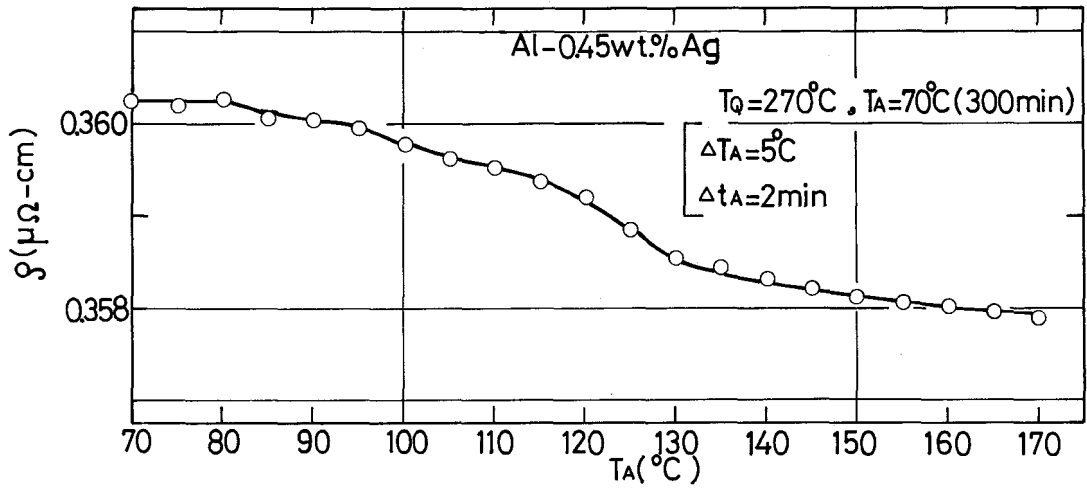


Fig.23 Isochronal curves of the 0.45%Ag alloy aged at 70°C for 300min after quenching from 270°C.

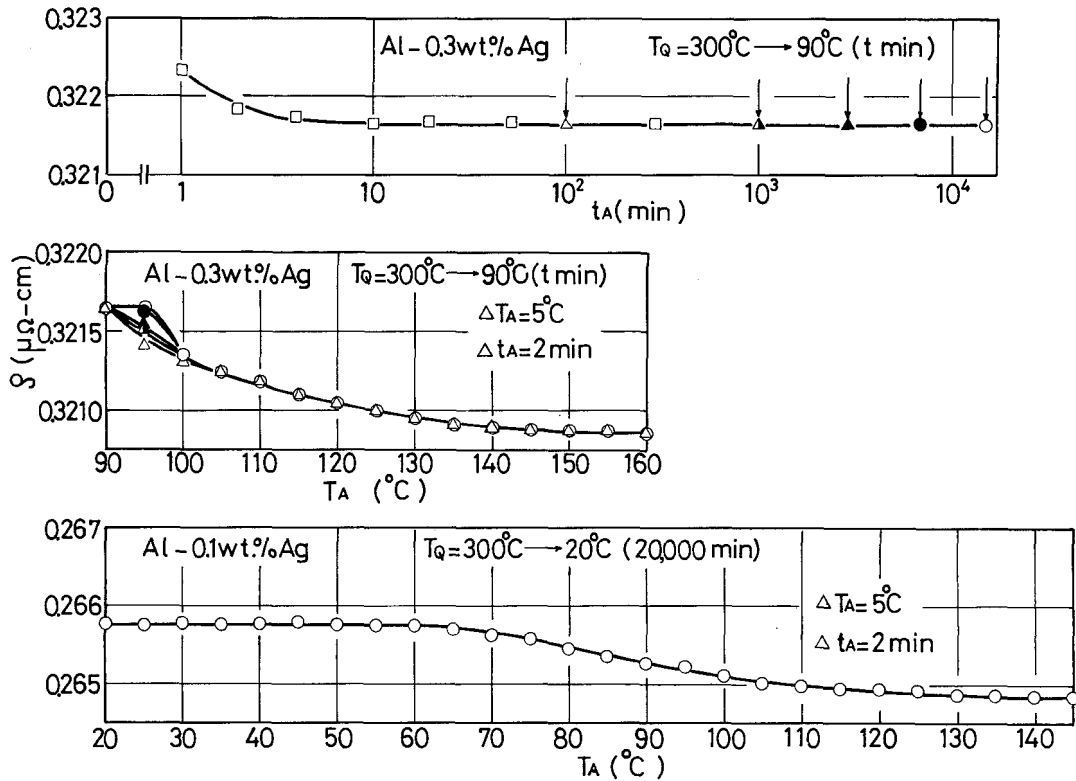


Fig.24 Isothermal annealing curves of the 0.3%Ag alloy at 90°C and isochronal curves after various annealing times at 90°C. At the bottom isochronal curves of the 0.1%Ag alloy after an isothermal annealing for 20000min at 20°C.



of G.P. zones.

The Al-0.3wt%Ag alloy was annealed isothermally at 90°C, the temperature higher than the spinodal temperature, for 100~15000min after quenching from 300°C and then annealed isochronally. The results are shown in Fig.24. Decrease of resistivity occurs in the same temperature range as that in Fig.22, between 90 and 105°C. Similar result was found also in Al-Zn alloys (11).

#### 4. Discussions

It has been well known that aging behaviors of Al-Ag alloys are very similar to those of Al-Zn alloys. Main differences between them are as follows: (1) Difference of atomic radius between solute and solvent atom is about 0.4% in Al-Ag alloys, but 4% in Al-Zn alloys and, in relation to this, spinodal temperature of Al-Ag alloys is relatively high even for low concentration. (2) G.P. zones become oblate ellipsoidal and change their structure to rhombohedral at the later stage of aging in Al-Zn alloys, on the other hand, the arrangement of atoms in G.P. zones becomes ordered to form  $\eta$ -phase in Al-Ag alloys. Present results will be discussed, with attention to these facts, by comparison with the results on Al-Zn alloys.

As for the fluctuation of concentration in dilute Al-Ag alloys, experimental study with isothermal annealing, as was carried out on Al-Zn alloy (3), is difficult because of the small variation in resistivity. However, the results in Fig.1 indicate that there is fluctuation in Al-Ag alloys at a relatively low temperature.

The results in Figs. 2~7 are almost the same as those found in Al-Zn alloys. It is considered that, when  $T_Q$  is high,  $\rho_{\max}$  is large because resistivity increase due to G.P. zones formed during quenching is added to that due to zones formed during aging by the spinodal decomposition (9). It is probably due to the effect of the fluctuation existing at  $T_Q$  that  $\rho_{\max}$  is small when  $T_Q$  is low. This effect will be mentioned later. The reason why resistivity does not take maximum but apparently stops changing in the case when  $T_Q=200^\circ\text{C}$  in Figs. 2, 5, 6 and 7 cannot be explained at present. If it is true that the fluctuation narrows the breadth of the distribution of the sizes of G.P. zones formed by the spinodal decomposition, the results above can be well explained, but methods to prove this supposition cannot be found at present. The fact that two-step aging occurs when, for instance,  $T_Q=250^\circ\text{C}$  in Fig.5, will be mentioned later.

The results in Figs. 8~18 and in Figs. 19~21 extremely resemble those of Al-10wt%Zn alloy (12). It was considered in Al-Zn alloys

that fluctuation reached the equilibrium state at  $T_{Q2}$  in a short time (20sec) after quenching from  $T_{Q1}$  to  $T_{Q2}$  ( $T_{Q1}$ :250~400°C,  $T_{Q2}$ :110~230°C). Vacancy concentration decreased during the holding at  $T_{Q2}$  to the equilibrium value at  $T_{Q2}$ . From various stages on the way, alloys were quenched again into iced water and aged at low temperatures. It was revealed by measurements of the intensity of small-angle X-ray scattering(SAXS) that, in Al-Zn alloys, the distribution of the sizes of G.P. zones is broad when the specimen is held for a short time at  $T_{Q2}$  and it becomes narrow with further longer time of holding. When the isothermal aging curve indicated two-step increase, profile of the scattering intensity curve had a maximum at each stage of aging. Such results of Al-Zn alloys were explained in terms of the rate and the limit of the low-temperature aging in the regions of higher and lower concentration (C and D regions) induced by fluctuation and in terms of the dependence of the rate and the limit on vacancy concentration.

The present results on Al-Ag alloys could be explained in a similar manner. As was done with Al-Zn alloys, two alloys of different composition, which are homogeneous but have much higher vacancy concentration than that in the present case, are compared, because it is difficult to obtain a homogeneous alloy in which vacancy concentration is so low as is realized in C and D regions after holding at  $T_{Q2}$ . When Fig.5 is compared with Fig.6, it is found that the alloy of higher concentration reaches  $\rho_{\max}$  earlier and shows more increase of resistivity than that of lower concentration. It has been known on Al-Zn alloys that, in the same alloy, Guinier radius of G.P. zones becomes smaller as the value of  $\rho_E$  (metastable value of resistivity found after  $\rho_{\max}$  in the isothermal aging curve) becomes larger (8). Difference between  $\rho_{\max}$  and  $\rho_E$  may be a measure of the limit of the growth of G.P. zones. It is more significant in the alloys of higher concentration.

It is expected that isothermal aging behavior should be a superposition of the effects of the alloys of different concentration when there is fluctuation in the alloy. When the quenching temperature is low, fluctuation exists in the alloy and aging in C regions is faster than that in D regions. When the alloy as a whole reaches at  $\rho_{\max}$ , G.P. zones in C regions become large but those in D regions remain small, which probably results in the small value of  $\rho_{\max}$ . When the quenching temperature is low and aging temperature is high, two-step aging is observed. This is also due to the fluctuation of concentra-

tion. When the aging temperature is high, supersaturation of solute concentration is small and the effect of the fluctuation may increase, that is, difference in the rate of aging in C- and D-regions may be large. Final size of G.P. zones may not be so large even in C regions. G.P. zones in D region continue growing after those in C region reach their final sizes, and then two-step aging may occur. Although solute concentration probably does not differ so much between C- and D-regions, the difference in the aging behavior between the two regions can be measured because of the low vacancy concentration.

Volume of the C- and D-region is unknown. It was reported (13) that the volume was relatively large ( $\sim 10^4 \text{Å}^3$ ) in the concentrated Al-Zn alloys, but no study has been carried out on the volume in dilute alloys. There is little information about Al-Ag alloys but the rate of growth of the amplitude is probably larger in C regions than in D regions when G.P. zones are formed by the spinodal decomposition, therefore the interpretation above mentioned may be true although the volume of the region is rather small. The volume of the region may be such as contains at least several G.P. zones in it.

In Fig.22, only the 1st stage of reversion occurs for a short aging time but, with longer aging, the 2nd stage increases while the 1st decreases and, moreover, the 3rd stage appears. The amount of the 1st and 2nd stage varies with aging time in the same manner as was observed in Al-Zn alloys. It has been found in Al-Zn alloys that G.P. zones reverted at the temperature just above the spinodal temperature (1st stage) have indefinite surfaces, and that those reverted in the 2nd stage, which increases with increasing aging time, have definite surfaces (11).

In Fig.24 reversion occurs in the same temperature range as that of the 2nd stage in Fig.22. Such a result has been found in Al-Zn alloy (11). It may be considered that G.P. zones are formed by the nucleation-and-growth mechanism because this annealing is done above the spinodal temperature (5). These G.P. zones, judging from the reversion temperature, may be the same as those with definite surfaces which are formed by the spinodal decomposition and reverted in the 2nd stage. In Al-Ag alloys, the 3rd stage is found in Fig.22 for the specimen aged for 100min after quenching from 400°C. This is probably due to  $\eta$ -zones in which ordering develops.

The authors wish to record their thanks to Messrs. H. Yamashita and A. Matsuwaka for assistance in the preparation of this paper.

## References

- (1) P. S. Rudman and B. L. Averbach: *Acta Met.*, 2(1954), 576.
- (2) A. J. Perry: *Acta Met.*, 14(1966), 1143.
- (3) M. Ohta, T. Kanadani and H. Maeda: *J. Japan Inst. Metals*, 40 (1976), 1199(in Japanese).
- (4) A. Junqua, J. Mimault, J. Delafond and J. Grilhe: *Scripta Met.*, 8(1974), 317.
- (5) J. Delafond, A. Junqua, J. Mimault and J. P. Riviere: *Acta Met.*, 23(1975), 405.
- (6) A. Naudon and A. M. Frank: *phys. stat. sol. (a)*, 41(1977), 207.
- (7) M. Ohta: *J. Japan Inst. Metals*, 27(1963), 197(in Japanese).
- (8) M. Ohta and F. Hashimoto: *J. Japan Inst. Metals*, 36(1972), 321 (in Japanese).
- (9) M. Ohta and F. Hashimoto: *J. Japan Inst. Metals*, 34 (1970), 700 (in Japanese).
- (10) M. Ohta, T. Kanadani, M. Yamada and A. Sakakibara: to be published.
- (11) M. Ohta, T. Kanadani, A. Sakakibara and M. Yamada: *J. Japan Inst. Metals*, 42(1978), 954(in Japanese).
- (12) M. Ohta, M. Yamada, T. Kanadani, M. Hida and A. Sakakibara: *J. Japan Inst. Metals*, 42(1978), 946(in Japanese).
- (13) H. Terauchi, N. Sakamoto, K. Osamura and Y. Murakami: *Trans. JIM*, 16(1975), 379.